Influence of Boron on the Decomposition of Austenite in Low Carbon Alloyed Steels

Ph. MAITREPIERRE, D. THIVELLIER, AND R. TRICOT

The influence of boron on the isothermal decomposition of Fe-Ni_6-$C_{0.12}$ (wt pct) steels has been investigated. The isothermal $\gamma \rightarrow$ pro-eutectoid ferrite reaction was studied by quantitative metallography and dilatometry. It was clearly shown that boron slows down considerably the nucleation rate of ferrite on γ-grain boundaries. End-quench experiments performed on $C_{0.18}$-Cr-Mn industrial steels emphasized the changes in hardenability with thermal history.

Particular attention was devoted to the study of the state and location of boron in the microstructure of the steels studied. Ion microscopy, alphagraphy and transmission electron microscopy were used to this effect. It was confirmed that boron segregates easily to γ-grain boundaries during cooling, which results in the precipitation of iron boro-carbides. This precipitation was shown to occur both in stable and metastable austenite, prior to the $\gamma \rightarrow$ pro-eutectoid ferrite reaction. The precipitates were identified as $Fe_{23}(B, C)_6$ (FCC structure with a ≈ 10.6Å). The grain boundary $Fe_{23}(B, C)_6$ were shown to have a parallel cube-cube orientation relationship with one of the neighboring grains. The role of the $Fe_{23}(B, C)_6$ precipitates with respect to the $\gamma \rightarrow$ proeutectoid ferrite reaction is discussed.

THE peculiar role of boron with respect to austenite decomposition in medium and low carbon steels has been a subject of research for at least 30 years. The potent effect[1] of minute additions of boron (a few tenths ppm, in wt pct) on hardenability offers one of the least expensive ways of improvement of the properties of a variety of steels. It is therefore hardly surprising that a strong interest[2,3,4,5] would develop for this addition at times when alloying elements are rare and/or expensive.

In spite of the obvious advantages of boron addition, users have often shown reluctance for boron-containing steels. Among various complaints, one of the essential ones was the seemingly nonreproducible effect of boron on hardenability. The lack of precise understanding of the role of boron throughout the processes of austenite decomposition was certainly a major stumbling-block. A considerable effort of research was therefore devoted to boron-containing steels in the 1950's,[6,7,8] but the results were somewhat unconclusive. The main reasons for this must certainly be found in the inherent difficulties of dealing with parts per million of an element of low atomic number (Z = 5). In recent years, the renewed interest for boron addition[4,5,9] and the general progress of methods of materials research have offered a new incentive for basic studies of the effect of boron on hardenability. In this framework a study of the effect of boron on austenite decomposition (essentially $\gamma \rightarrow$ pro-eutectoid ferrite transformation) was carried out in low carbon alloyed steels. Isothermal decomposition experiments and standard Jominy tests were conducted to assess hardenability. A particular emphasis was placed on the study of the location of boron in the microstructure after various heat treatments, which required the extensive use of transmission electron microscopy, alphagraphy and ion microscopy.

I — MATERIALS — EXPERIMENTAL PROCEDURE

1 — Materials

The study was carried out both on laboratory and industrial heats. The composition of the laboratory heats was selected so that the steels (even without boron) would have fairly large incubation times for the $\gamma \rightarrow$ pro-eutectoid ferrite reaction. This led to select Fe-Ni_6-$C_{0.12}$ alloys (with or without 50 ppm B - wt pct). The choice of nickel was brought about by the fact that this element is a known γ - stabilizer with no affinity for carbon and full solubility in Fe. The carbon concentration was chosen in the "low-carbon" range since it is well documented that the effect of boron is particularly intense in low-carbon steels. The full chemical compositions of these laboratory heats (steels A and B) are given in Table I (wt. pct).

These heats were vacuum melted and cast into 3 kg ingots which were homogenized at 1200°C (4 h) and rolled to 17×17 mm rods (finishing temperature ≈ 1000°C).

Two industrial heats were also selected for this study and their chemical compositions are given in Table II (steels IA and IB). They are Mn-Cr grades with C $\approx$ 0.18.

Table I. Composition of Laboratory Heats A and B, Wt Pct

	Ni	C	B	Al	N	O	Fe
Steel A	6.30	0.12	0.0	0.006	0.003	0.003	compl
Steel B	6.25	0.12	0.0050	0.005	0.003	0.002	compl

Ph. MAITREPIERRE is Research Engineer, Groupe Métallurgie Physique, Institut de Recherches de la Sidérurgie Française (IRSID), 78104 Saint Germain en Laye, France. D. THIVELLIER is Research Engineer and R. TRICOT is Director, respectively, Centre de Recherches d'Ugine-Aciers 73400, Ugine, France.

Manuscript submitted March 14, 1974

Table II. Composition of Industrial Heats IA and IB, Wt Pct

	C	Si	Mn	Ni	Cr	Mo	Al	B
Steel IA	0.185	0.235	1.24	0.296	0.942	0.027	0.012	<0.0005
Steel IB	0.174	0.237	1.25	0.294	0.929	0.028	0.07	0.0100

These heats were melted in an electric furnace and cast as 2.7 metric ton ingots. They were subsequently forged into Ø 32 mm bars (forging temperature in the range 1100 and 1200°C) and normalized 30 min. at 925°C.

2 — Heat Treatments — Kinetics Studies

The steels A and B were used to study the dissolution and precipitation of borides during austenitizing treatment. Various austenitizing temperatures, ranging from 900°C to 1250°C, were investigated. These experiments were performed on small samples (10 $\times 10 \times 2$ mm) which were water quenched after austenitizing. Precipitation studies were performed by step quenching such small samples at temperatures in the range 950 to 600°C.

The kinetics of the $\gamma \rightarrow$ pro-eutectoid ferrite were carefully investigated in steels A and B. Small samples ($10 \times 10 \times 2$ mm) were austenitized for 1 h, then isothermally held at 600°C for various lengths of time and quenched in water. Metallographic polished and etched (nital $\approx$ 2 pct) sections were subsequently used for the determination of transformation curves by quantitative metallography (quantimet B). A limited number of isothermal dilatometric experiments were also performed to verify the results obtained by quantitative metallography. Hand - countings on optical micrographs of appropriate magnification were also used for the determination of the average number of ferrite particles per unit area of a metallographic polished surface.

In steels IA and IB, the hardenability was determined by the standard Jominy test. Thermal treatments were performed on Ø 32 mm bars and a subsequent Jominy test was then performed on such samples (end-quenched with 850° - 30 min. austenitizing). The hardness measurements on the end-quenched Jominy samples were performed at a sufficient depth to avoid any interference from superficial decarburizing or deboronizing.

3 — Detection and Localization of Boron in Steel

This aspect of the study is essential for an improvement of the understanding of the effect of boron in steel. It was therefore most carefully considered in the course of this study. Since boron was present in the steels investigated at a concentration level of the order of a few tens ppm (wt pct), *i.e.*, a few hundreds ppm (atomic pct), methods exhibiting a specific sensitivity for boron, or trace sensitive in general, were required. The location of boron was therefore mainly studied by alphagraphy and secondary ion spectroscopy techniques. A limited number of Auger electron spectroscopy experiments were also conducted.

The method of boron autoradiography used is the fission track etching technique described by Hughes and Rogers.[10] Various authors have shown that the α particles resulting from the nuclear reaction

$$^{10}B\,(n^{th},\ \alpha)^{7}Li$$

(where n^{th} stands for thermal neutrons) could be easily detected by their damage tracks in cellulose nitrate[11,12] or cellulose acetobutyrate[10,13] (it must be mentioned here that "natural" boron such as that used to alloy the steels is a mixture of 81.2 pct ^{11}B and 18.8 pct ^{10}B). The autoradiographic method used in the course of the present work consisted in placing a cellulose nitrate film in close contact with a polished sample surface and irradiating the whole in a reactor (integrated flux $\approx 10^{12}\ n^{th}/cm^2$).

After exposure, the film was stripped from the metal and etched in an aqueous 10 pct NaOH solution at 60°C for 10 to 30 min. The etched film was then observed by means of optical microscopy (or scanning electron microscopy, after metallizing).

Secondary ion spectroscopy[14,15] is becoming an increasingly widespread technique for the detection (without atomic number limitation) of trace elements. The CAMECA secondary ion microprobe SMI 300 used during this study has a mass sensitivity of the order of 10^{-10} to 10^{-12} grams. This instrument easily permits the detection of boron in steels,[16] even at the ppm level. The CAMECA instrument, like various other ion microprobes, can be used to obtain filtered ion micrographs, which give the location of a selected element in the microstructure, with a resolution of 1 to 5 μm. Such micrographs are obtained from areas $\approx 250\ \mu$ in diam on the polished flat surface of the steel sample.

A limited number of Auger electron spectroscopy experiments were performed on intergranular rupture surfaces. The fractures were done *in-situ* in a Physical Electronics Auger Spectrometer and the Auger spectra obtained with a cylindrical mirror electron analyzer.

4 — Microstructure Characterization

This was carried out by standard optical microscopy, scanning electron microscopy and transmission electron microscopy (thin foils - replicas). A particular emphasis was put on the identification of precipitate phases by thin foil electron microscopy and selected area diffraction.

II — EXPERIMENTAL RESULTS

1 — Isothermal $\gamma \rightarrow$ Pro-eutectoid Ferrite Reaction Kinetics

The laboratory heats A and B have been used for a study of $\gamma \rightarrow$ pro-eutectoid ferrite reaction kinetics at 600°C (after 1100°C - 1 h austenitizing). The reaction temperature was selected, after preliminary experiments, as a temperature well suited for isothermal step-quenching experiments as well as isothermal dilatometry experiments. The austenitizing conditions were chosen after measuring the average γ - grain size. These measurements indicated that, after 1100°C - 1 h austenitizing, the γ - grain size was reproducible and similar in both steels (in fact, the mean grain diameter was about 10 pct larger in steel B). This temperature

was also deemed necessary to obtain complete dissolution of boron-containing precipitates (see below II.2).

The optical micrographs of Fig. 1 show that the ferrite formed at 600°C is of the "Widmanstätten" type and is grain boundary nucleated. The slowing-down effect of boron on the nucleation of pro-eutectoid ferrite is already apparent on these micrographs. The transformation kinetics were determined by dilatometry and quantitative metallography and the results are presented in Fig. 2. In this figure, the experimental results are normalized (100 pct transformation at 10^5 s). One can readily see the satisfactory agreement between dilatometry and quantitative metallography data. The retarding effect of boron on the $\gamma \rightarrow$ pro-eutectoid ferrite reaction is also quite obvious. The transformation curves are of the sigmoidal type, as is expected for a phase transformation involving nucleation and growth. A Johnson-Mehl analysis of these curves leads to the results presented in Fig. 3. These curves permit a clear distinction of the time-range of grain boundary nucleation prior to site saturation. Site saturation occurs for $\approx 10^3$ seconds in steel A and $5 \cdot 10^3$ s in steel B. Beyond site saturation, the exponent n of the Johnson-Mehl formula is of the order of 1 in both steels A and B.

In order to study more precisely the nucleation of the $\gamma \rightarrow$ pro-eutectoid ferrite reaction (which is essential as far as hardenability is concerned), the average number of ferrite particles per unit area of a polished and etched sample, was determined by hand-counting on optical micrographs. The results of these measurements are shown in Fig. 4. It is difficult to evaluate a true volume nucleation rate from the number, N, of nuclei counted per unit area on a plane of polish. It was therefore decided to determine a two-dimensional nucleation rate N_S such as:

$$N_S = \frac{1}{1 - X(t)} \cdot \frac{dN}{dt}$$

where $X(t)$ is the fraction of austenite transformed. The variation of N_S with time is shown in Fig. 5. For all observable conditions, N_S decreases rapidly with time in steel A, whereas it goes through a maximum at an intermediate reaction time in steel B. It is clear that boron greatly decreases the rate of grain boundary

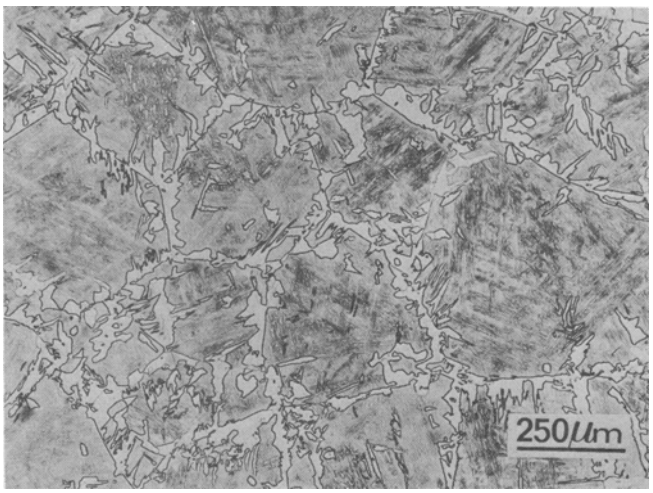

Steel A

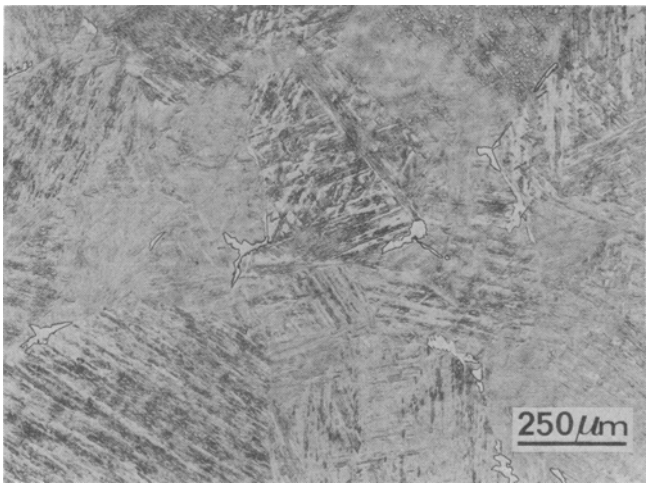

Steel B

Fig. 1—Optical micrographs of samples of steel A and B partially reacted at 600°C for 10^3 s, after 1100°C - 1 h austenitizing.

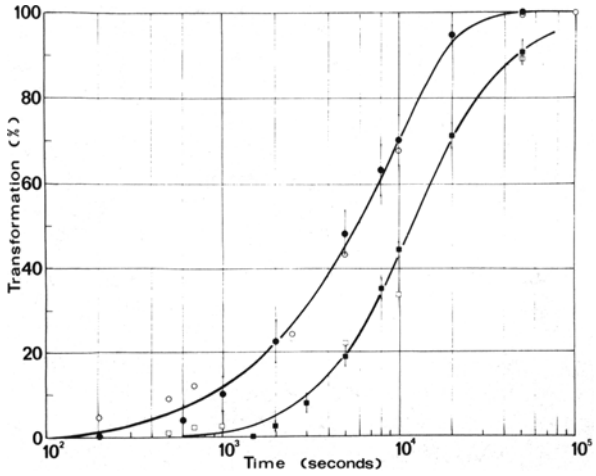

Fig. 2—Isothermal transformation curves of steels A and B at 600°C (1100°C - 1 h austenitizing).
—Quantitative metallography: Steel A (○)
Steel B (□)
—Dilatometry: Steel A (●)
Steel B (■).

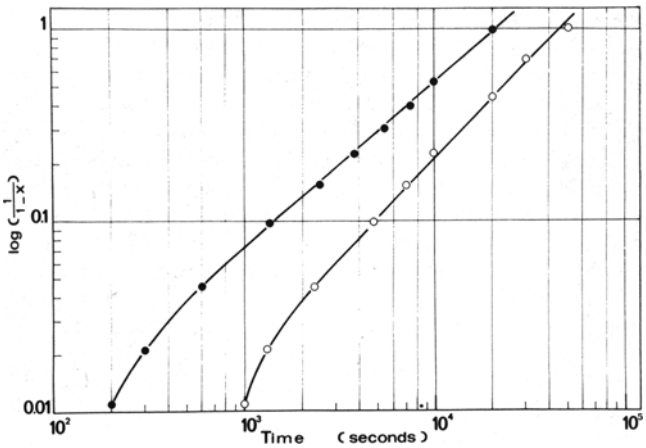

Fig. 3—Isothermal $\gamma \rightarrow$ pro-eutectoid ferrite reaction at 600°C (after 1100°C - 1 h austenitizing): Johnson-Mehl plot. (Steel A [●] - Steel B [○]).

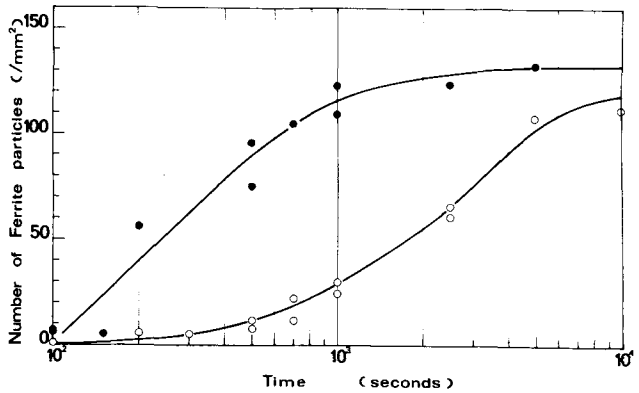

Fig. 4—Average number of ferrite particles per unit area of polished metallographic surface, as a function of reaction time at 600°C (1100°C austenitizing); Steel A (●) - Steel B (○).

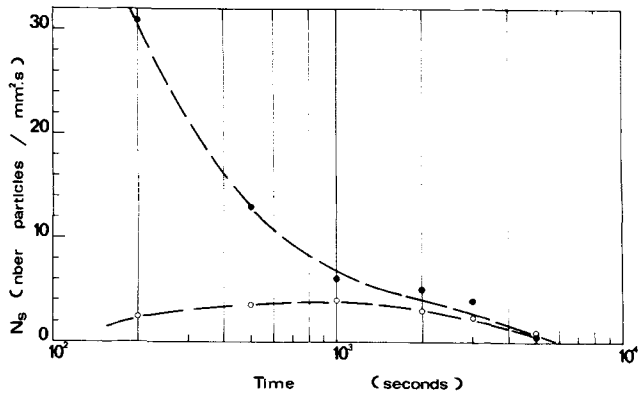

Fig. 5—Nucleation rate at 600°C for Steel A (●) and Steel B (○).

nucleation of ferrite, but that, for times of the order of site saturation, the number of ferrite particles is not substantially different in both steels. It seems, therefore, that boron does not drastically change the average number of nucleation sites (at least in the present case).

A limited number of experiments concerning the isothermal $\gamma \rightarrow$ pro-eutectoid ferrite reaction were conducted at 650°C on the industrial steels IA and IB. These experiments again confirmed the inhibiting effect of boron on the grain boundary nucleation of ferrite.

The austenitizing temperature was set at 1100°C in the experiments just described. However, austenitizing temperature is an essential parameter of grain boundary nucleated transformation such as the $\gamma \rightarrow$ pro-eutectoid ferrite reaction. It was therefore decided to investigate the influence of this parameter on the overall decomposition kinetics. In order to achieve this purpose, the complete transformation curves at 600°C were determined after various austenitizing conditions and the average γ - grain size was measured on optical micrographs of suitably etched samples. From these two-dimensional measurements, an average three dimensional γ - grain size, $\bar{D}$, was obtained from the classical formula:

$$\bar{D} = 1.55/(N_A)^{1/2}$$

(where N_A is the number of grains per unit area on the plane of polish).

To appreciate and compare the various austenitizing temperatures, the transformation kinetics were characterized by an appropriate "incubation time" τ, namely the time necessary to reach 10 pct transformation at 600°C. The complete set of results in presented in Fig. 6 where τ is plotted versus $\bar{D}$. These data show conclusively that τ is always substantially larger in the boron-containing steel than in the boron free steel, for a given austenitic grain size. This is true up to the largest γ-grain sizes (corresponding to austenitizing 1 hour at 1200°C). It is worth noting, however, that the effect of boron on hardenability is more noticeable for small γ-grain sizes, where the relative variation of τ is larger than that observed for larger grain sizes. This remark emphasizes a general observation according to which boron is most effective for low austenitizing temperatures.

2 — End-quench Experiments

This part of the study concerns only the industrial steels IA and IB. The main purpose of these experiments was to show the effect of a previous heat treatment on the Jominy hardenability. The end-quench tests were all carried out after austenitizing at 850°C for 30 min. The results obtained are presented in Figs. 7 and 8. In all cases, the hardenability was measured by the hardness J20 (Rockwell C) at 20 mm from the quenched-end. The influence of a previous austenitizing treatment (followed by water quenching) is shown in Fig. 7. Whereas the hardenability is hardly changed in the B-free steel, a decrease with increasing austenitizing temperature was observed in the B-containing steel. However, the austenitizing time did not appear to affect the results. It was found that the loss of hardenability of the B-containing steel was not erased by a second austenitizing treatment at low temperature (925°C - 30 min.) prior to the Jominy test.

The effect of cooling after austenitizing on the hardenability of steel IB is described in Fig. 8. It is observed that, whereas the hardenability of the B-free

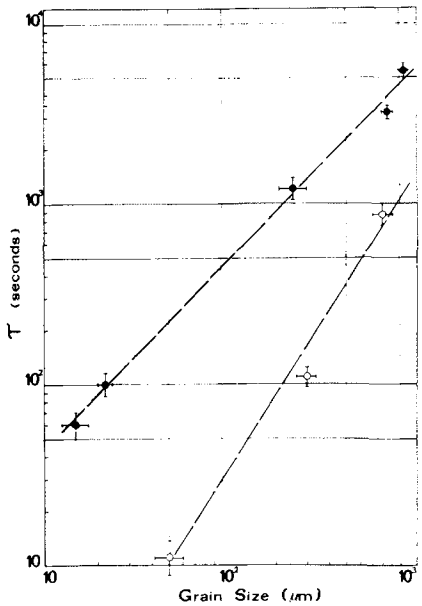

Fig. 6—Variation of incubation time τ with average γ-grain size $\bar{D}$: Steel A (○) - Steel B (●).

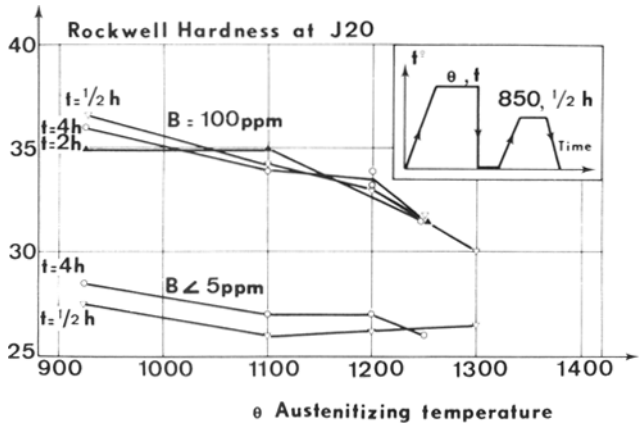

Fig. 7—Influence of a previous austenitizing treatment on the Jominy hardenability of Steels IA and IB.

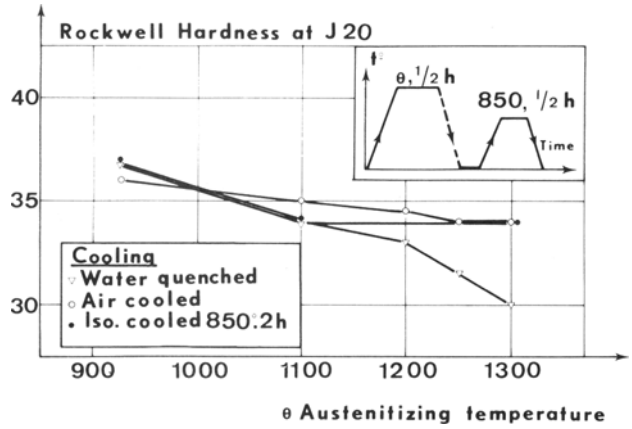

Fig. 8—Influence of cooling after austenitizing on the Jominy hardenability of Steel IB.

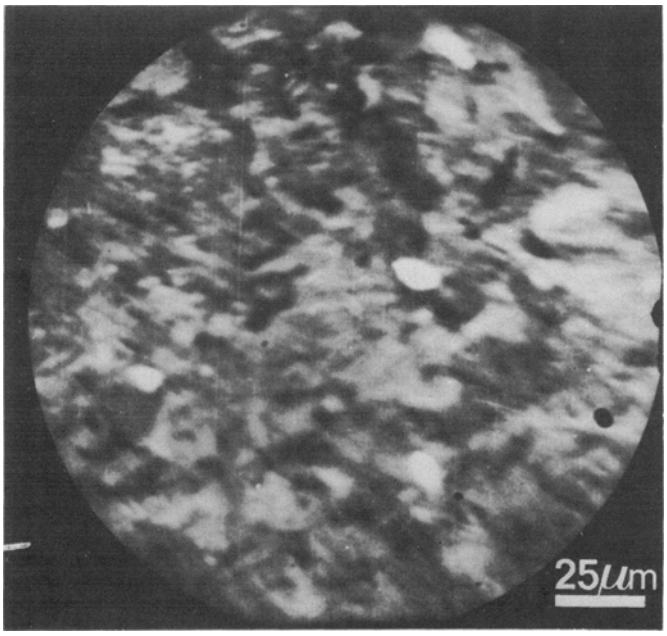

(a) $^{56}Fe^{+}$

Fig. 9—Steel B, austenitized 1 hour at 1000°C and water-quenched. Ion micrographs, with secondary $^{56}Fe^{+}$, $^{11}B^{+}$ and $^{12}C^{+}$ ions (O_2^{+} primary).

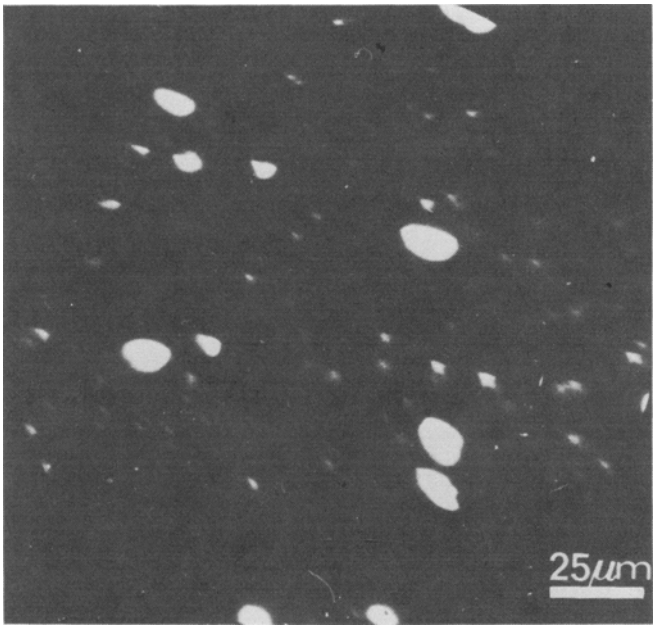

(b) $^{11}B^{+}$

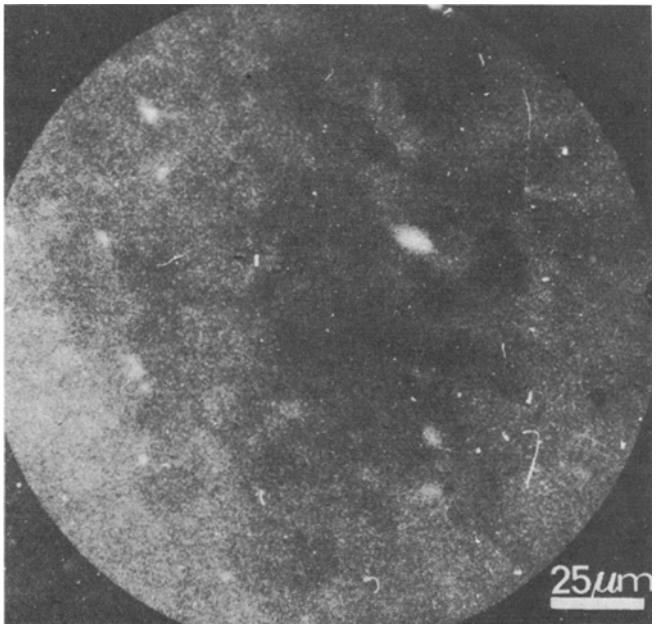

(c) $^{12}C^{+}$

steel IA isnot noticeably affected, measurable effects appear in the case of steel IB. The detrimental influence of the austenitizing temperature is more pronounced in the case of water quenching than in the case of slow cooling or step-cooling.

The end-quench experiments reveal therefore the prime importance of the prior thermal (and, certainly, thermomechanical) history of the B-containing steel to be tested by a standard Jominy experiment.

3 — Microstructure — Boron Location

This essential part of the study was mainly concerned with: the dissolution of borides during austenitizing, the precipitation of borides during cooling and

the location of boron in the microstructure of isothermally decomposed samples.

a) Dissolution of boron in austenite: This problem was studied by ion microscopy on samples rapidly quenched from various austenitizing temperatures (1 h - 900 to 1250°C). Small samples (2 mm thick) of all four steels investigated had fully martensitic structures after water quenching (the martensite would usually contain fine cementite particles indicative of quench-tempering).

The austenitizing and quenching treatments were performed essentially on steel B. A typical set of ion micrographs is shown in Fig. 9 (1000° austenitizing temperature). The $^{56}Fe^{+}$ ion micrograph has a poor contrast but confirms the fully martensitic structure of the as-quenched sample. The $^{11}B^{+}$ micrograph reveals the presence of both large and small boron-containing particles. The $^{12}C^{+}$ micrograph indicates that carbon is present in those large particles. The $^{56}Fe^{+}$ image also seems to indicate the presence of Fe in the same particles. It is therefore logical to assume that these

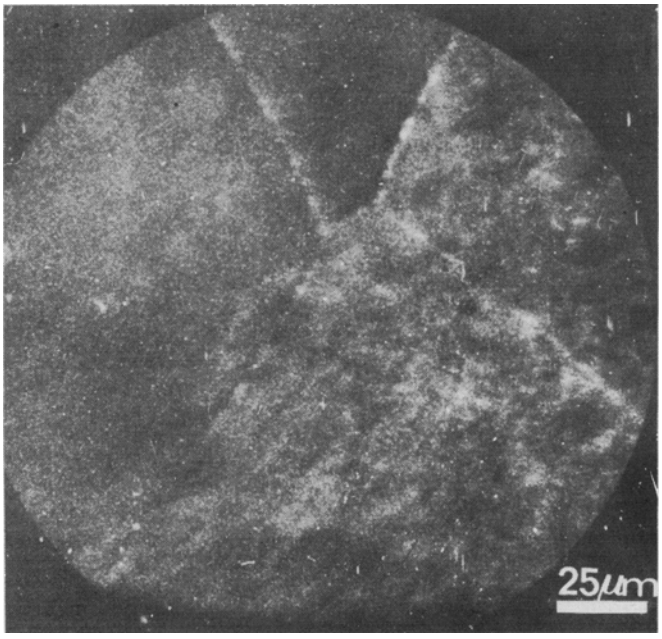

$^{11}B^{+}$

Fig. 10—Steel B, water-quenched from 1250°C - 1 h austenitizing. Secondary $^{11}B^{+}$ ion micrograph (O_2^{+} primary ions) revealing grain-boundary borides.

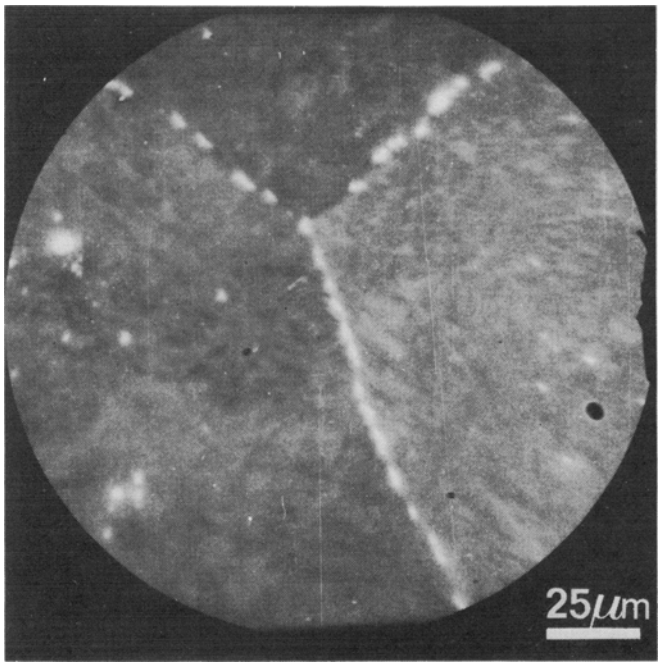

(a) $^{56}Fe^{+}$

Fig. 11—Steel B: step-quenching 1100°C - 1 h → 750°C - 1 h + water-quenching. Ion micrographs, with secondary $^{56}Fe^{+}$, $^{11}B^{+}$ and $^{12}C^{+}$ ions (O_2^{+} primary ions) showing large grain-boundary boro-carbides.

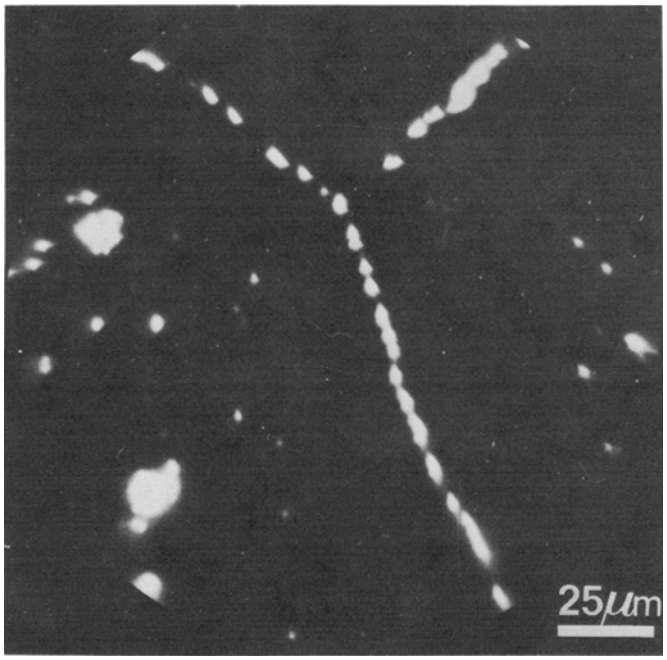

(b) $^{11}B^{+}$

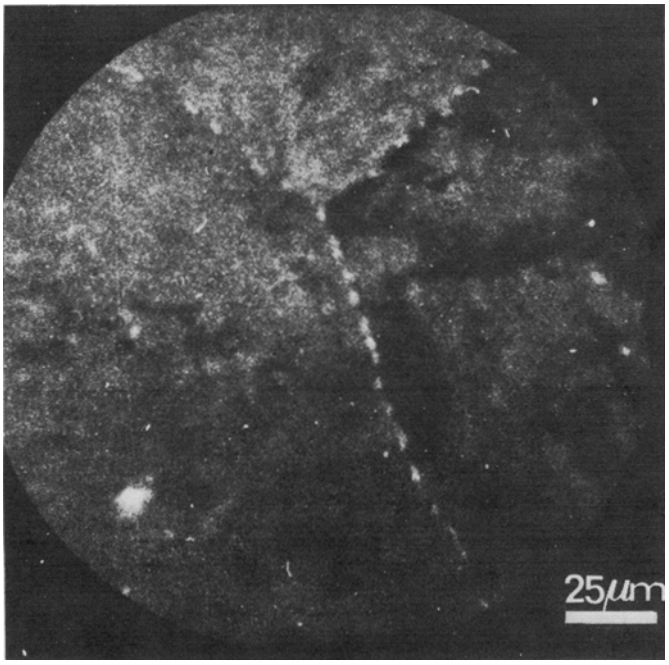

(c) $^{12}C^{+}$

large boron-containing particles were undissolved at 1000°C (and below). The origin of the smaller borides apparent on the $^{11}B^+$ image will be discussed later in this paper. Upon raising the austenitizing temperature to 1100°C, one no longer observes the large boron-containing particles. This seems to indicate a complete dissolution of those borides above 1000°C. However, after austenitizing at high temperature (1100°C and above) a fine borides precipitation along γ-grain boundaries was clearly observed after water-quenching (Fig. 10).

From these ion microscopy experiments on martensitic quenched samples of steel B, the following points can be emphasized:

—for low austenitizing temperatures, large borocarbides stay undissolved.

—with the composition of steel B, complete dissolution is obtained between 1000° and 1100°C.

—precipitation of borides along γ-grain boundaries can occur even during water-quenching from high austenitizing temperatures.

b) Precipitation of borides on γ-grain boundaries: Since the dissolution of boron could be considered complete at 1100° in steel B, a number of experiments were performed to ascertain the temperature range of the borides precipitation on γ-grain boundaries during cooling, as well as the precise nature of these borides.

Step-quenching experiments in the stable austenitic range, followed by ion microscopy observations, revealed that the precipitation of borides occurs rapidly below $\approx$ 950°C. Typical ion micrographs are shown in Fig. 11. The precipitates there are rather coarse, because of the long holding time, and are easily observable also by optical microscopy. For shorter times the $^{11}B^+$ ion micrographs are similar to that shown in Fig. 10. The $^{56}Fe^+$, $^{11}B^+$ and $^{12}C^+$ images shown in Fig. 11 again suggest that the grain boundary precipitates (long known as "Boron-constituent"[1,17]) are iron boro-carbides.

A complete crystallographic identification of the precipitate boride phase was carried out by transmission electron microscopy on extraction replicas and thin foils, in spite of experimental difficulties (easy dissolution of the borides in the usual etching and polishing solutions). A typical thin foil electron micrograph is shown in Fig. 12. Selected area diffraction patterns indicated that the precipitates had an FCC lattice with a $\approx$ 10.6Å. This permitted their identification as the iron boro-carbide $Fe_{23}(B, C)_6$. This borocarbide was originally identified by Carrol, Darken *et al.*[18] in the course of a study of the Fe-B-C phase diagram. The "Boron-constituent" was also recently identified as $Fe_{23}(B, C)_6$ in various low carbon steels.[19,20] The $Fe_{23}(B, C)_6$ boro-carbide is isomorphous to the well known $M_{23}C_6$ carbide and its lattice parameter is also approximately three times that of austenite.

It is well established that the $M_{23}C_6$ carbide nucleate with a parallel (cube-cube) orientation relationship with the parent austenite (in Cr-Ni stainless steels for instance).[21,22] It was therefore considered particularly important to verify whether such an orientation relationship existed for $Fe_{23}(B, C)_6$ precipitating in the austenite of carbon steels. Unfortunately, for such steels, austenite is not directly observable, unless by hot stage

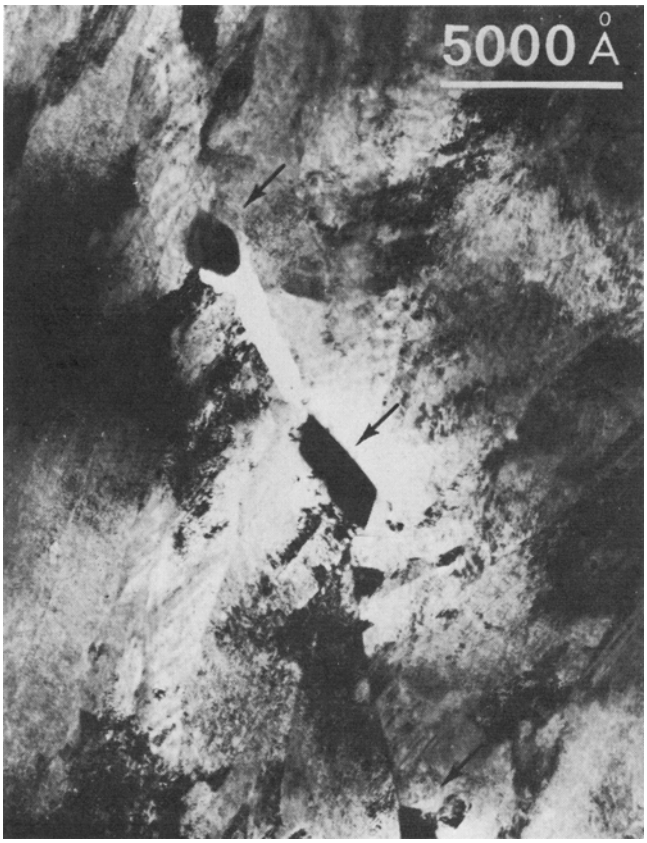

Fig. 12—Steel B: step-quenching 1100°C - 1 h → 600°C - 5000 seconds + water-quenching. Transmission electron micrograph showing grain-boundary $Fe_{23}(B, C)_6$ borocarbides) in an untransformed (fully martensitic) area.

microscopy. An alternate way is to determine the orientation relationship between $Fe_{23}(B, C)_6$ and martensite lattices. If one assumes that martensite and parent austenite are related by a Kurdjumov-Sachs[23] orientation relationship, it is then possible to determine the $Fe_{23}(B, C)_6$-austenite orientation relationship. It is worth noting here that since one is dealing with grain boundary precipitates, the orientation relationship (if any) should exist with one of the former γ-grains and not with the neighboring grain across the boundary.

Selected area diffraction patterns, such as that shown in Fig. 13, revealed a definite orientation relationship between the FCC lattice of $Fe_{23}(B, C)_6$ and the BCC lattice of a set of martensite plates on one side of the former γ-grain boundary. This was confirmed by the joint use of selected area diffraction patterns and dark field micrography. In the example described in Figs. 13 and 14, a grain boundary $Fe_{23}(B, C)_6$ precipitate formed in steel IB by isothermal holding at 850°C for 2 h (austenitizing 1300°C – 30 min.) is shown to have its (111) plane exactly parallel to the (110) plane of a set of martensite plates. Moreover, the reciprocal lattice planes $(1\bar{1}1)^*_{\text{martensite}}$ and $(1\bar{1}0)^*_{Fe_{23}(B, C)_6}$ are approximately parallel (Fig. 13). The orientation relationship between martensite and $Fe_{23}(B, C)_6$ can then be summarized as:

$$(111)_{Fe_{23}(B, C)_6} \parallel (110)_{\text{martensite}}$$

$$[1\bar{1}0]_{Fe_{23}(B, C)_6} \parallel [1\bar{1}1]_{\text{martensite}}$$

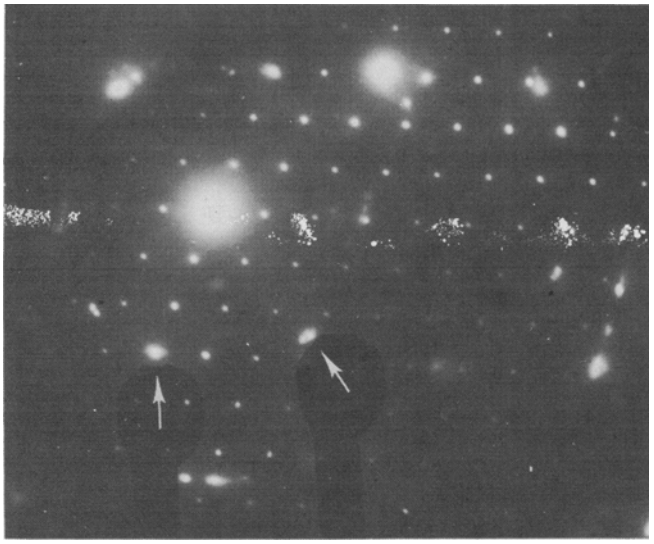

(a)

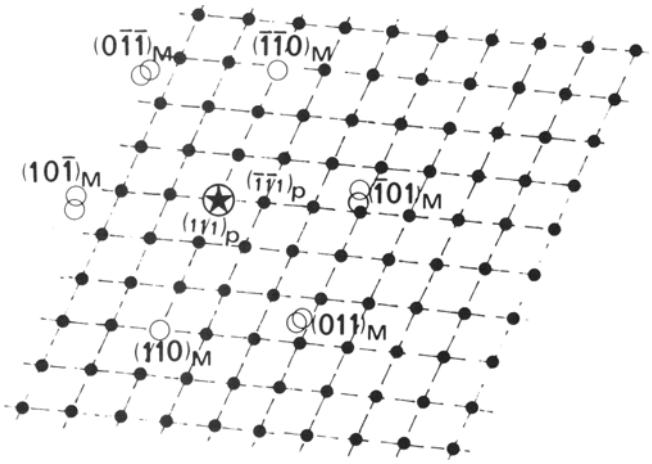

(b)

Fig. 13—Selected area diffraction on a grain-boundary boride in Steel I B (step-quenching 1300°C - $\frac{1}{2}$ h → 850°C - 2 h + water-quenching).
—(*a*) — Experimental diagram.
—(*b*) — Indexation showing the Kurdjumov-Sachs orientation relationship.

This is the Kurdjumov-Sachs (K-S) relationship between FCC and BCC lattices. If one then assumes that a similar relationship holds between parent austenite and martensite, it can be safely deduced that the two FCC lattices of austenite and $Fe_{23}(B, C)_6$ are parallel (cube-cube relationship). This is, of course, true only on one side of the γ grain boundary (Fig. 14).

c) $\gamma \rightarrow$ pro-eutectoid ferrite decomposition: The location of boron in the microstructure of samples of steel B partially reacted at 600°C was investigated. As mentioned earlier, the pro-eutectoid ferrite formed in steels A and B after austenitizing as 1100°C consist essentially of Widmanstätten "saw-teeth" and blocky allotriomorphs, according to the Dubé-Aaronson classification.[24,25]

For holding times too short for ferrite nucleation, ion micrographs (Fig. 15) clearly reveal a grain boundary segregation of boron in what appears to be distinct particles: the $^{56}Fe^+$ micrograph of Fig. 15 shows a fully martensitic structure, whereas the $^{11}B^+$ image indicates

(a)

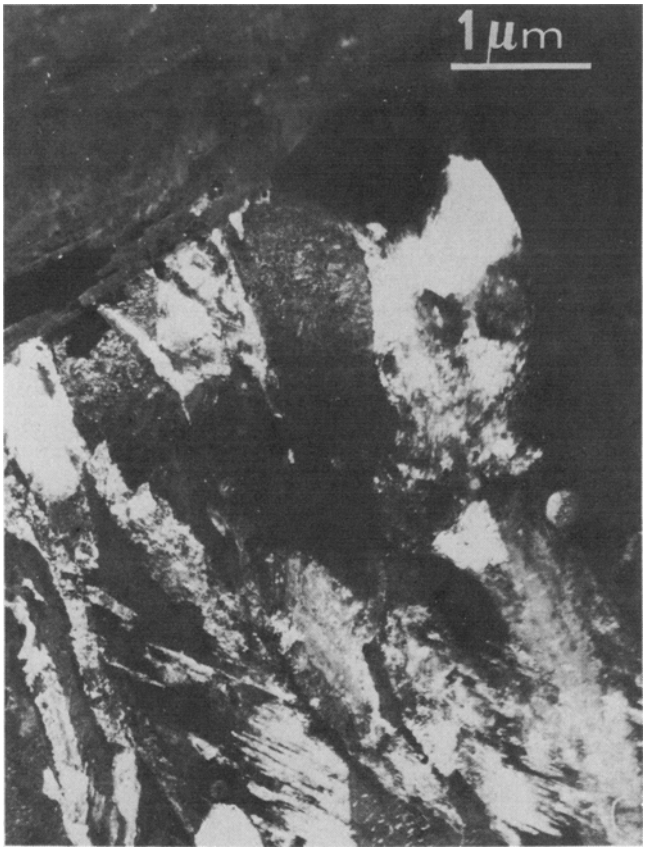

(b)

Fig. 14—Steel I B (same as Fig. 13); Dark field images with: -a - $(110)_M$ and $(333)_{Fe_{23}(B,C)_6}$ (common spot). -b - $(011)_M$.

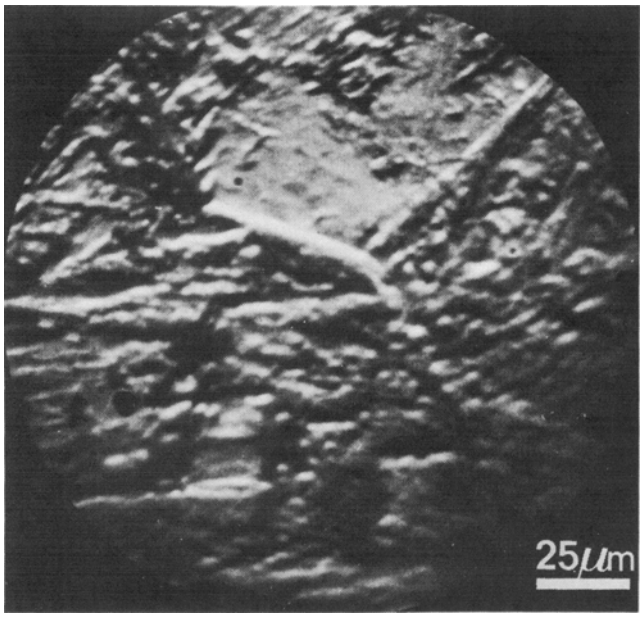

(a) $^{56}Fe^{+}$

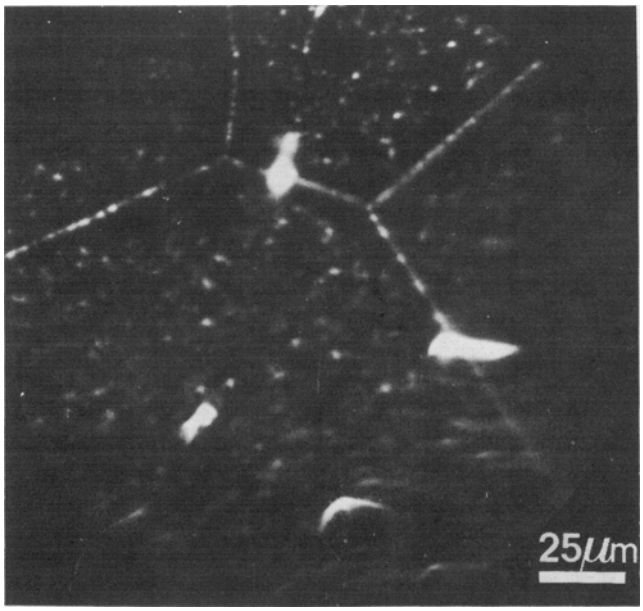

(b) $^{11}B^{+}$

Fig. 15—Steel B untransformed after 300 seconds holding at 600°C (1100°C austenitizing). Ion micrographs with secondary $^{56}Fe^{+}$ and $^{11}B^{+}$ ions (O_2^{+} primary ions).

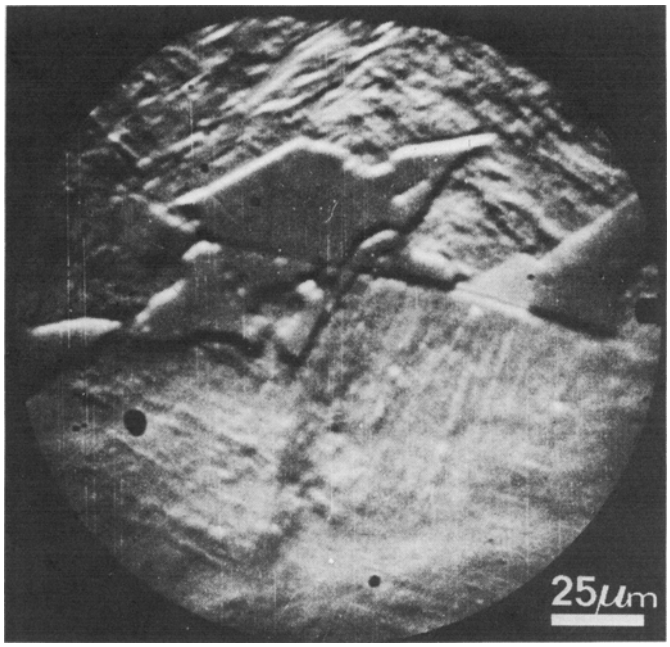

(a) $^{56}Fe^{+}$

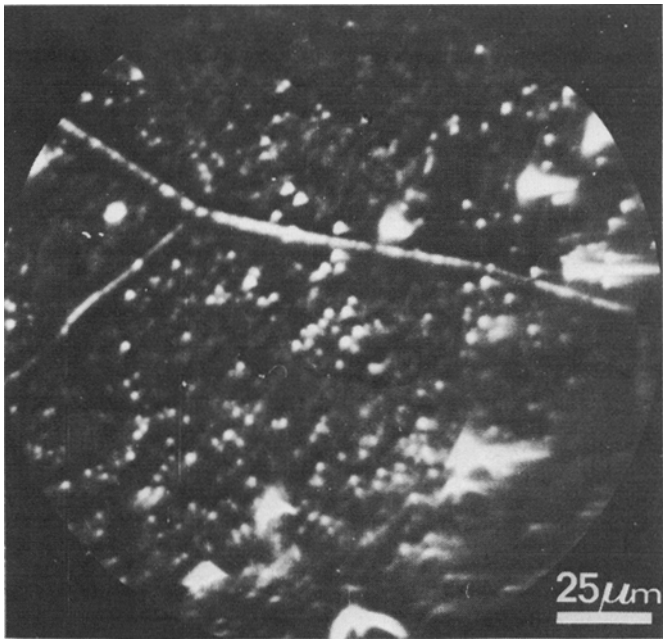

(b) $^{11}B^{+}$

Fig. 16—Steel B partially transformed after 10^4 s holding at 600°C (1100°C austenitizing). Ion micrographs with secondary $^{56}Fe^{+}$ and $^{11}B^{+}$ ions (O_2^{+} primary ions).

the presence of borides on γ-grain boundaries and also inside the grains. There appears to be a boron-free zone (a few μm thick) on both sides of the γ-grain boundaries.

After holding times sufficient to reach the $\gamma \rightarrow \alpha$ transformation range, ion micrographs such as those shown in Fig. 16 are obtained. The $^{56}Fe^{+}$ images reveal clearly the two phase martensite-ferrite microstructure and the $^{11}B^{+}$ images are quite similar to those obtained for shorter holding times (compare Fig. 16 with Fig. 15). Boron-autoradiographs, such as that shown in Fig. 17, confirm the grain boundary "segregation" of boron in partially reacted samples but do not have a sufficient resolution to reveal individual borides. Thin foil transmission electron microscopy on partially reacted samples of steel B showed (Fig. 18) the presence of grain boundary borides (suggested by the ion micrographs). Selected area diffraction confirmed that they were $Fe_{23}(B, C)_6$. It is also worth noting here that the morphology of those grain boundary $Fe_{23}(B, C)_6$ precipitates is akin to that of $M_{23}(B, C)_6$ in austenitic Cr-Ni steels and $Fe_{23}(B, C)_6$ precipitates in Fe-Ni_{36}-B austenitic steels.[26]

In numerous instances (both in steels B and IB), it was observed that the grain boundary boro-carbides seemed to inhibit the development of ferrite on one side of the γ-grain boundary (Figs. 19 and 20). A similar observation was made by Ohmori.[19] The observed

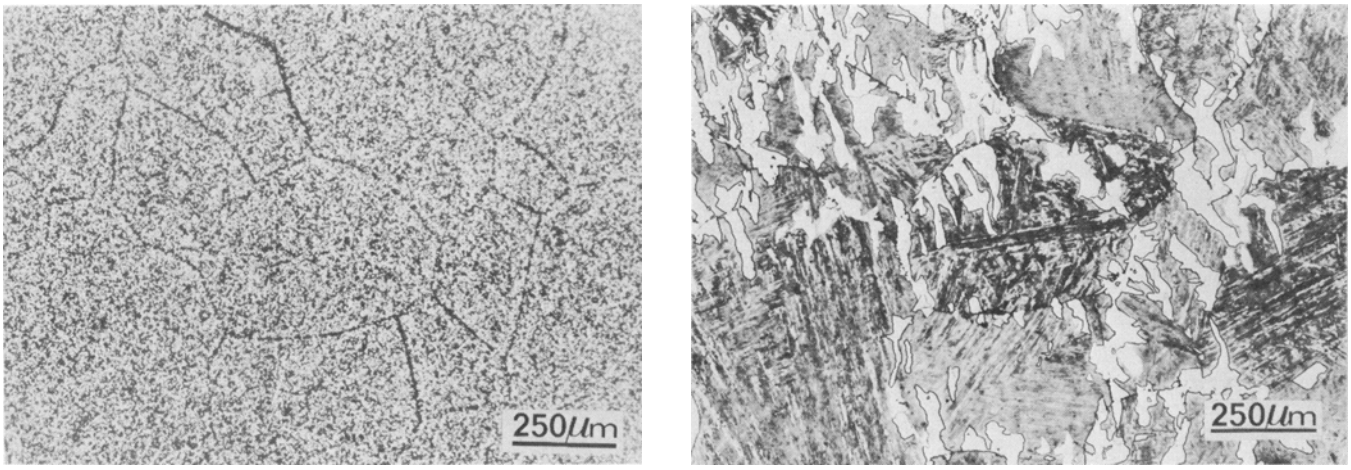

(a) (b)

Fig. 17—Boron alphagraph (*a*) and related optical micrograph (*b*). Steel B partially transformed at 600°C (1100°C - austenitizing).

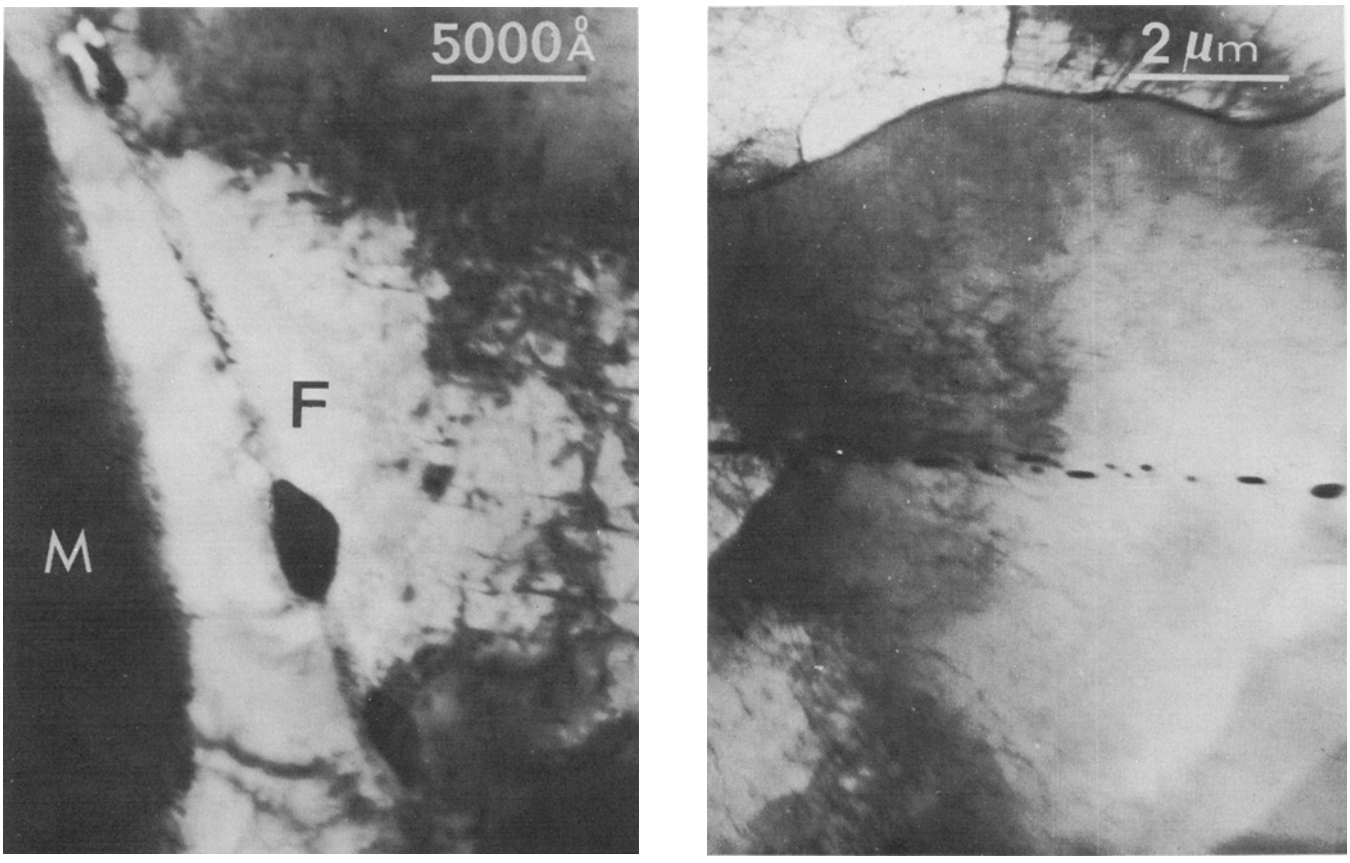

(a) (b)

Fig. 18—Thin foil transmission electron microscopy on Steel B, partially transformed at 600°C. Micrographs showing $Fe_{23}(B, C)_6$ along former γ-grain boundaries in martensitic-ferritic (*a*) and fully ferritic (*b*) areas.

"occultation" is a result of inhibited nucleation and growth of ferrite. It was however possible to show that this "occultation" occurs on the side of the γ-grain with which the $Fe_{23}(B, C)_6$ precipitate is semi-coherent. This point is of particular importance as far as the role of those precipitates with respect to the $\gamma \rightarrow$ pro-eutectoid ferrite reaction is concerned.

III — DISCUSSION

1 — Behavior and Distribution of Boron in Austenitic Phase

A precise knowledge of the state and distribution of boron in austenite is the key to the understanding of the effect of boron on austenite decomposition. The

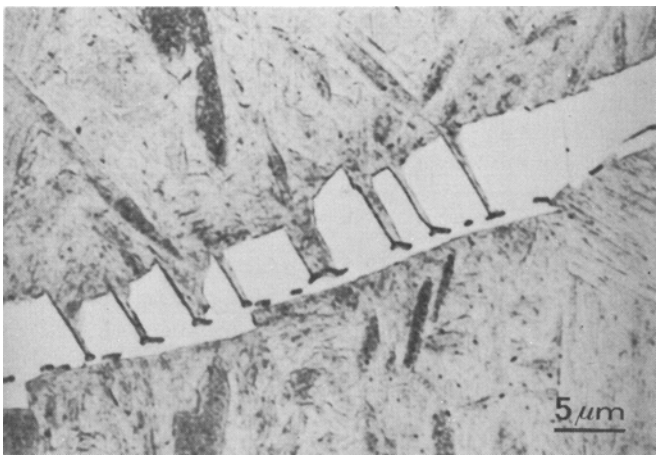

Fig. 19—Steel I B isothermally reacted at 650°C for 4 min. (1300°C - ½ h austenitizing). Optical micrograph showing occultation of ferrite by grain boundary $Fe_{23}(B,C)_6$ precipitates.

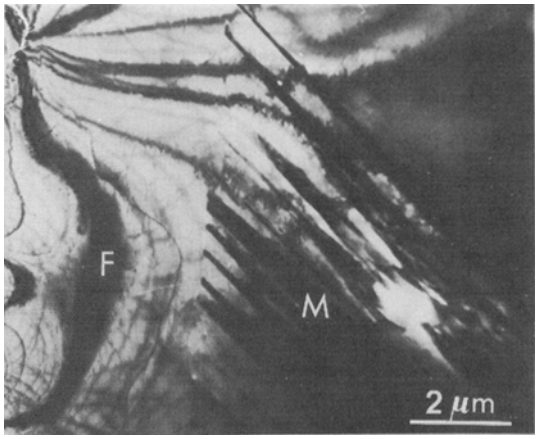

Fig. 20—Steel B, isothermally reacted at 600°C for 5000 seconds. Transmission electron micrograph showing the occultation of ferrite (F) by grain-boundary $Fe_{23}(B,C)_6$ precipitates (M = martensite).

main results of the present study are relative to the dissolution of boron-containing phases during austenitizing and to the segregation and precipitation of boron at austenitic grain boundaries during cooling. Ion micrography experiments (such as those presented in Fig. 9) demonstrate that, at low austenitizing temperatures ($T \leq 1000°$), some large boron-containing precipitates were not dissolved. The smaller borides present on the $^{11}B^+$ image of Fig. 9 can probably be attributed to precipitation during cooling. The nature and amount of the undissolved particles has not been precisely determined in the course of this study. It is, however, clear, from correlated ion micrographs, that these particles are iron boro-carbides, formed during the previous thermomechanical history of the steel studied. The existence of such undissolved borides has been reported by various authors,[17,19] who are in general agreement on their nature ($Fe_{23}(B,C)_6$ and/or $Fe_3(B,C)$). An appropriate technique of phase analysis would be highly desirable so as to make possible a measure of the amount of boron present in these undissolved boro-carbides. Various experimental procedures have been proposed to this effect[28,29] and developments should be forthcoming.

For austenitizing temperatures above 1000°C, it was noticed that the coarse iron boro-carbides were dissolved. However, rapid cooling could not prevent some segregation of boron to grain boundaries in what appears to be individualized precipitates. The whole question of segregation of boron to γ grain boundaries is still fairly unsettled. The two main problems are:

a) whether grain boundary segregation occurs at high austenitizing temperature or during cooling.

b) whether the grain boundary segregation of boron is in a truly "atomic" form or in the form of borides.

Concerning item (a), the interpretation of experiments is conflicting. An essential aspect of this problem lies in our impricise knowledge about the type of solid-solution Fe_γ-B and the equilibrium diagrams Fe-B[30,31,32] and Fe-C-B. It seems, however, likely that boron exists in some type of interstitial solution in austenite,[33] probably in close association with vacancies so as to accommodate its unusually large atomic radius. Various recent experimental results [34,35] suggest some type of "boron atoms-vacancies" interaction. Concerning the segregation of boron to austenite grain boundaries, Simcoe *et al.*[6] believe that an increased grain boundary adsorption of boron occurs with increasing temperature. This would, according to these authors, speed up the precipitation of borides during subsequent cooling. This interpretation is disputed by Grange and Mitchell,[17] and various authors [36,37] who notice that the amount of boron segregated (in atomic or precipitate form) increases with decreasing cooling rate (from a given austenitizing temperature). For instances, Ueno and Inoue[37] using an alphagraphy technique, showed that boron segregation was undetectable in a low carbon steel (containing 5 ppm B) quenched in helium gas from 1350°C, but that clear grain boundary segregation was observed after air-cooling from the same austenitizing temperature. Similar experiments were performed by the authors of the present paper, both on carbon steels and an austenitic $Fe\text{-}Ni_{36}\text{-}B_{0.008}$ steel. In the latter case,[26] no boron segregation could be observed (by ion microscopy) after water quenching of small samples from 1200°C, but evidence of grain boundary borides could be seen in air cooled and furnace-cooled samples. A further argument towards the segregation of boron during cooling has been put forward by Grange and Mitchell[17] who showed that, in a deformed and recrystallized steel, the new grain boundaries were the ones to which boron segregated during cooling or holding at an intermediate temperature. Similar observations were made by Dulieu and Irani.[38] The existence of a boron-free zone on both sides of γ-grain boundaries, after step-quenching treatments (as shown in Fig. 15 for instance), is also indicative of a rapid migration of boron during cooling. Such a rapid and complete migration is likely to be due to a vacancy-aided diffusion.

Whatever be the final answer to question a), the important fact is still that boron is present in substantial amounts at the austenite grain boundaries, in the temperature range of interest for austenite decomposition. Various attempts have been made to distinguish a true "atomic" segregation of boron from a fine precipitation of borides. The difficulties of that task are multiple and satisfactory experiments have yet to be devised. The shortcomings of most experiments have been that they relied on a single technique of charac-

terization of boron segregation (selective etching, alphagraphy, optical metallography). For instance, it is highly questionable whether one can differentiate "segregated" boron from "precipitated" boron by alphagraphy, contrary to recent published data.[37] Careful electron microscopy observations coupled with alphagraphy and ion micrography reveal indeed the limitation of low magnification techniques such as alphagraphy. For instance the fission track-etching alphagraph of Fig. 17 does not permit a distinction between "segregated" or "precipitated" boron, when electron microscopy observations (Fig. 18) reveal the presence of individual borides. On the other hand; C-curves for borides precipitation, such as those drawn by Grange and Mitchell,[17] are too dependent on the limited scale of observation provided by optical microscopy. Consequently, the boundaries of such precipitation curves are at best approximative and do not give any information on the presence of a zone of "atomic" boron segregation, if it exists. Auger electron spectroscopy on intergranular rupture surfaces should be an attractive technique as far as detecting an eventual "atomic" segregation of boron.[39] The difficulty is to perform the Auger analysis on the relevant surface (*i.e.*, to make sure the surface is wholly intergranular). The few experiments performed in the course of the present study showed a clear B peak on intergranular rupture surfaces of samples with grain boundary borides already observable by electron microscopy.

The present study has dwelt on identifying the grain boundary borides which precipitate for temperatures below approximately 950°C. These precipitates have long been known as "boron-constituent" and the present study, as well as recent published results, shows that they are iron boro-carbides $Fe_{23}(B, C)_6$, with an FCC lattice and a ≈ 10.6Å. The existence of this compound was first mentioned by Darken *et al.*[18] as one of the various phases in the Fe-B-C phase diagrams. More recent investigations[40,41] indicate that their lattice parameter can vary from 10.58 to 10.62Å when the ratio B/B + C increases. The precision of the electron diffraction patterns obtained in the course of our study was not adequate to determine the value of this ratio. It is likely, however, that the formula is closer to $Fe_{23}B_6$ than $Fe_{23}C_6$ in the case of the steels studied.

The orientation relationship between the FCC lattices of $Fe_{23}(B, C)_6$ and the parent austenite grain was shown to be of the parallel (cube-cube) type. Ohmori[19] has recently reached a somewhat different conclusion, namely that there existed a twin-relationship between $Fe_{23}(B, C)_6$ and austenite. All the results of the present investigation indicate however the parallel relationship only. Such a relationship is well documented for the $M_{23}C_6$ carbide in Cr-Ni austenitic stainless steels. Singhal and Martin,[22] for instance, have shown that grain boundary nucleated $M_{23}C_6$ precipitates bear a cube-cube relationship with one or other of the two grains bordering the grain boundary. Kegg and Silcox[42] have recently shown that the ratio r of corresponding atomic positions in austenite and $M_{23}C_6$ is high. It was shown to be highest for {111} planes ($r = 0.78$) and still large for {110} and {100} planes. The interface between precipitate and parent austenite is therefore often {111} and recent electron microscopy observations[43] have shown that such semi-coherent interfaces contain interfacial dislocations. Since $Fe_{23}(B, C)_6$ is isomorphous to $M_{23}C_6$ and has also a lattice parameter very close to three times that of austenite, it is hardly surprising that it would nucleate with the parallel cube-cube relationship. No extensive trace analysis was carried out in the low carbon steels to determine the crystallographic nature of the interface with the matrix. It is however likely that the nature of the interface is of the same type as that of $M_{23}C_6$ in austenitic steels. Another evidence of this is the "puckering" of the grain boundary due to the precipitation of $M_{23}C_6$ and $Fe_{23}(B, C)_6$. This is indicative of a low energy interface between the grain boundary precipitates and a neighboring grain.[44,45]

It is worthwhile to mention here that the precipitation of $M_{23}(B, C)_6$ (with M = Fe, Cr) is a general feature of boron-containing austenites. Besides Cr-Ni stainless steels and carbon steels, this precipitation was also observed in austenitic Fe-Ni_{36}-B alloys.[26]

2 — $\gamma \rightarrow$ Pro-eutectoid Ferrite Transformation — Hardenability

The experiments conducted in the course of this study confirm the large effect of boron on austenite decomposition kinetics.

The isothermal kinetics study of $\gamma \rightarrow$ pro-eutectoid ferrite decomposition in steel A and B (base Fe-Ni_6-$C_{0.12}$) shows clearly that boron diminishes considerably the nucleation rate of ferrite on γ grain boundaries (Figs. 4 and 5). This observation is in agreement with the conclusions reached by Simcoe *et al.*[6] and is essential to explain the effect of boron on hardenability. A careful examination of the data presented in Figs. 2 and 4 shows that the number of nucleation sites is not noticeably affected by the presence of boron. This can be further demonstrated by plotting the number of ferrite particles measured on a polished section versus the amount of transformation (Fig. 21). It is therefore the activation of ferrite nucleation which is affected by boron. The formula generally put forward for the ferrite grain boundary nucleation rate N_γ can be written as:[25]

$$N_\gamma = K \exp - \left[\frac{\pi (3\sigma_{\gamma\alpha} - \sigma_{\gamma\gamma})^3}{3 (\Delta F_V + \Delta F_S)^2} + \Delta F_D \right] \Big/ RT$$

where:

— $\sigma_{\gamma\gamma}$ and $\sigma_{\gamma\alpha}$ are the interfacial energies for γ/γ and γ/α interfaces.

— ΔF_V is the volume free energy change accompanying the formation of ferrite.

— ΔF_S is the volume strain energy attending the appearance of embryos of ferrite.

— ΔF_D is the free energy of activation for the diffusion of carbon.

Most theories proposed so far to explain the influence of boron on ferrite nucleation on γ-grain boundaries have tended to look for a change in the surface energy term or in the diffusion term ΔF_D to explain the effect of boron. It is indeed quite unlikely that such minute concentrations of boron would greatly affect ΔF_V, as pointed out by Sharma and Purdy in a recent paper.[46]

Various authors[6,33,37] have proposed a mechanism

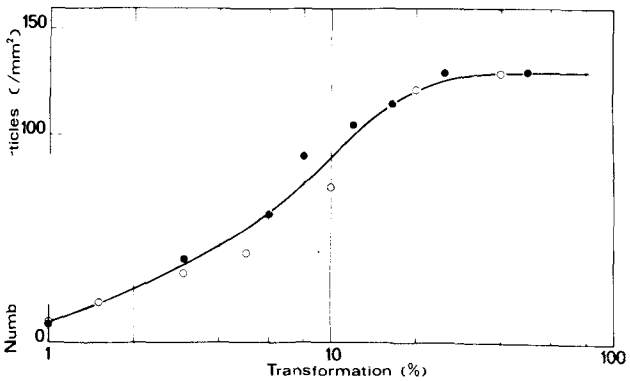

Fig. 21—Average number of ferrite particles per unit area of polished metallographic surface as a function of transformation (pct) at 600°C. Steel A (●) - Steel B (○) (data are corrected to take into account the small γ-grain size differences between both steels, after 1100°C austenitizing).

which assumes that boron segregation (in an "atomic" form) lowers the energy of γ-grains boundaries enough to account for the inhibition of ferrite nucleation. It has further been generally assumed and stated that, when boron-containing precipitates form consecutively to the "atomic" segregation, the inhibiting effect should decrease.[6,20,37] This idea proceeded from the rationale that any grain boundary phase would necessarily provide extra nucleation sites. The serious limitations relative to the mechanism involving an "atomic" degregation of boron reside in the lack of definite experimental evidence. Even the recent extensive study (using alphagraphy) of Ueno and Inoue[37] falls short of providing a clear distinction between "effective" boron "segregated" or "precipitated" as fine precipitates. On another hand, various studies which attributed a loss of effectiveness of boron to the precipitation of grain boundary borides are notoriously limited by the resolution of the methods used (mainly optical microscopy).

The present study has shown that a clear inhibiting effect of boron on the nucleation of ferrite existed during the 600°C isothermal decomposition of austenite of the Fe-Ni_6-$C_{0.12}$ steels, after austenitizing at 1100°C. It was also shown that, in the same conditions, $Fe_{23}(B, C)_6$ precipitated as fine particles on γ grain boundaries before the onset of the $\gamma \rightarrow \alpha$ reaction (Figs. 15 and 16). It was therefore felt that an essential part of the problem lies within the role such grain boundary particles might play with respect to the nucleation of ferrite, at a later time. The precipitates being $Fe_{23}(B, C)_6$ and having nucleated in parallel orientation with the parent γ-grain, the interface between the precipitate and that grain is therefore of substantially reduced energy when compared to the energy of the γ grain boundary. It is therefore expected that the nucleation of ferrite could be inhibited on that side of the grain boundary. This is indeed experimentally observed (Figs. 19 and 20). The other interface of the precipitate (with the neighboring γ-grain) is fully incoherent and can be considered as having an energy of the order of the grain boundary energy itself (several hundred ergs/cm²). Therefore, if the precipitates are small enough so that they do not provide large extra areas of incoherent boundaries, the net result can be an inhibition of the ferrite nucleation (when compared to a boron-free steel). This situation should progressively be altered by thecoarsening of the grain boundary $Fe_{23}(B, C)_6$ precipitates.

The case of multiple nucleation on grain boundaries has been discussed by Nicholson[47] who emphasized the importance of the nature of the interface between the first nucleated phase and the parent matrix. Very recently, in a review article on ferrite nucleation, Sharma and Purdy[46] have put forward a mechanism of inhibition of ferrite nucleation by grain boundary $Fe_{23}B_3C_3$ borocarbides which is essentially that proposed by the authors of the present article. Sharma and Purdy also emphasized that the grain boundary boro-carbides could act as nucleation-inhibiting agents at early reaction times and favor ferrite nucleation when they have coarsened. This latter point was also supported by the results of the present study. In order to emphasize the importance of the size and distribution of grain boundary $Fe_{23}(B, C)_6$ precipitates, a series of isothermal decomposition experiments was performed on steel B, with or without intermediate holding at 800°C for 20 h (this intermediate treatment provoked a coarsening of grain boundary precipitates as shown in Fig. 22). A comparison of reaction rates at 600°C (Fig. 23) reveals a clear effect of the holding at 800°C, which leads to an increase in transformation rate (a loss in hardenability). It appears, therefore, that large coalesced borides have less of an inhibiting effect than finer ones. A similar observation was made by Ueno and Inoue.[37]

The influence of austenite grain size on the $\gamma \rightarrow$ proeutectoid ferrite reaction kinetics (at 600°C) was briefly discussed in the presentation of the results summarized in Fig. 6. These results show clearly that, in steel B, the inhibiting effect of boron existed for all austenite grain sizes, *i.e.*, for all austenitizing temperatures investigated (up to 1250°C). The apparently smaller slope of the τ vs $\bar{D}$ line observed in steel B seems to be a general feature of boron-containing steels.[48] An explanation for this behavior must be looked for in variations in size and distribution of grain boundary borides according to austenitizing temperature.

The end-quench experiments conducted on steels IA

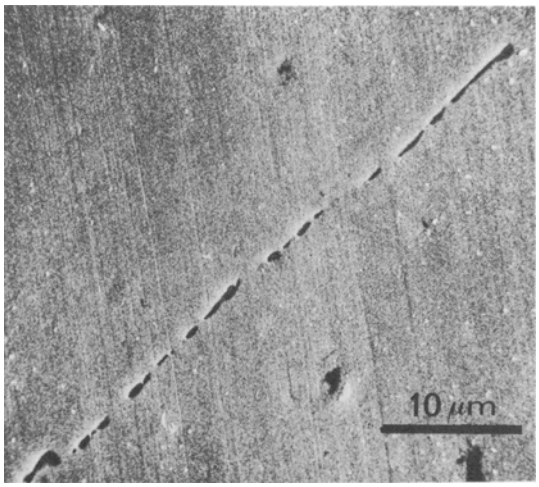

Fig. 22—Grain-boundary $Fe_{23}(B, C)_6$ precipitates formed by isothermal holding 20 h at 800°C. Scanning electron micrograph (secondary electrons) on a polished and lightly etched (Nital 1 pct) sample of steel B.

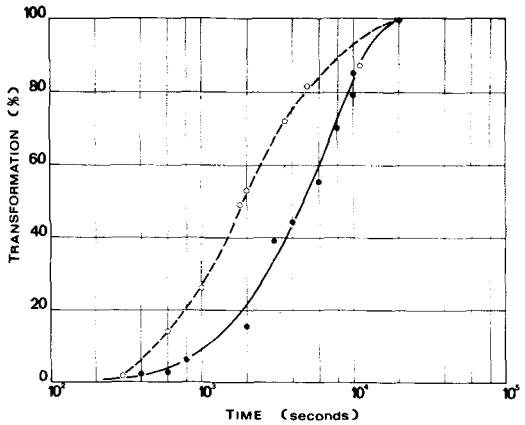

Fig. 23—Steel B: Isothermal reaction curves at 600°C (austenitizing 1050°C). No intermediate holding: (●). Intermediate holding (20 h - 850°C): (○).

and IB underline the prime importance of the thermal (and thermomechanical) history of the boron-containing steel, as far as hardenability is concerned. When the hardenability is measured after low-temperature austenitizing (such as 850°C in the present case) it is now clear that precipitated borides will not be dissolved. The available boron concentration in solid solution is therefore quite dependent on the previous heat treatment. Moreover, the amount and distribution of undissolved borides is also highly dependent on that history. One expects that this would have a direct influence on the rate of austenite decomposition during a subsequent treatment (such as an end-quench test from 850°C). For instance, it is likely that undissolved fine borides would then be more detrimental for hardenability (*i.e.*, catalytic of ferrite nucleation) than large coalesced borides. The variations of hardenability apparent in Figs. 7 and 8 could be explained by such a rationale.

IV — CONCLUSIONS

The study of the isothermal reaction $\gamma \rightarrow$ pro-eutectoid ferrite in Fe-$Ni_6C_{0.12}$ steels has confirmed the strong inhibiting effect of boron on the grain boundary nucleation of ferrite.

The precipitation of borides at γ-grain boundaries was extensively investigated and the results can be summarized as follow:

— The precipitates are $Fe_{23}(B, C)_6$ with an FCC lattice and a parameter $a \approx 10.6$Å.

— The precipitates nucleate in austenite with a parallel (cube-cube) orientation relationship with one of the neighboring grains.

— The range of precipitation of $Fe_{23}(B, C)_6$ during cooling covers both stable austenite ($T < 950$°C) and metastable austenite.

The role of the grain boundary $Fe_{23}(B, C)_6$ precipitation with respect to the $\gamma \rightarrow$ pro-eutectoid ferrite reaction was discussed and it was suggested that, contrary to a general acceptance, these precipitates could have an inhibiting effect on ferrite nucleation. It is however clear that the whole question of the effect of grain boundary borocarbides on hardenability will not be settled definitely until critical particle size and distribution are determined and related to optimum boron concentrations.

Finally, the great influence of the thermal and thermomechanical history of boron-containing steels on their hardenability was emphasized.

Further work is however needed to reach a completely satisfactory understanding of the mechanisms necessary to explain the effects of boron. Progress is likely to depend on the developments of new methods of characterization and microanalysis of materials. Research in this field should stay lively in the years to come due to the development of boron-containing steels, which are made increasingly attractive by the general price increase of alloying elements.

ACKNOWLEDGMENTS

The authors are indebted to Mr. Barbier (Kodak Laboratories) for the boron-alphagraphy tests and to the Cameca Company for the experiments conducted with the SMI 300 ion microprobe.

They thank MM. Champin, Henriet, Henry, Rofes-Vernis and Thomas for many helpful discussions and MM. Leray and Lionnet for their assistance in the experiments.

Part of this study was financed by the C.E.C.A. Authority.

REFERENCES

1. R. A. Grange and T. M. Garvey: *Trans. ASM,* 1946, vol. 37, p. 136.
2. T. H. Spencer: *Metal Prog.,* Nov. 1966, p. 76.
3. G. F. Melloy and J. C. Russ: *Metal Prog.,* Nov. 1966, p. 83.
4. J. M. Calkins and C. A. Dennis: *Electric Furnace Proc. AIME,* 1969, vol. 27, p. 71.
5. G. F. Melloy: Bethlehem Steel Co., Bethlehem, Pa. Communication no. 263 presented at the TMS–AIME Meeting, Chicago, Oct. 1973.
6. C. R. Simcoe, A. R. Elsea, and G. K. Manning: *Trans. AIME,* 1955, vol. 203, p. 193 and *Trans. AIME,* 1956, vol. 206, p. 984.
7. K. J. Irvine, F. B. Pickering, W. C. Heselwood, and M. Atkins: *J. Iron Steel Inst.,* 1957, vol. 186, p. 54.
8. J. C. Fisher: *Trans. AIME,* 1954, vol. 200, p. 1146.
9. R. Tricot, B. Champin, and D. Thivellier: *Rev. Met.,* 1972, vol. 69, p. 121.
10. J. D. Hughes and G. T. Rogers: *J. Inst. Metals,* 1967, vol. 95, p. 299.
11. J. S. Armijo and H. S. Rosenbaum: *J. Appl. Phys.,* 1967, vol. 38, p. 2064.
12. S. Kawasaki, A. Hishinuma, and R. Nagasaki: *J. Nucl. Mater.,* 1971, vol. 39, p. 166.
13. J. D. Hughes, M. A. Dewey, and G. W. Briers: *Nature,* Aug. 1969, vol. 223, p. 498.
14. R. Castaing: Comptes rendus du IVè Congrès International sur l'Optique des Rayons X et la Microanalyse. Herman, Paris, p. 48, 1966.
15. G. Slodzian: *Rev. Phys. Appl.,* 1968, vol. 3, p. 360.
16. Ph. Maitrepierre and R. Tixier: IRSID Internal Report RI 168, June 1971.
17. R. A. Grange and J. B. Mitchell: *Trans. ASM,* 1961, vol. 53, p. 157.
18. K. G. Carroll, L. S. Darken, E. W. Filer, and L. Zwell: *Nature,* Nov. 1954, vol. 174, p. 978.
19. Y. Ohmori: *Trans. I.S.I. Jap.,* 1971, vol. 11, p. 339.
20. G. F. Melloy, P. R. Slimmon, and P. P. Podgursky: *Met. Trans.,* 1973, vol. 4, p. 2279.
21. M. H. Lewis and B. Hattersly: *Acta Met.,* 1965, vol. 13, p. 1159.
22. L. K. Singhal and J. W. Martin: *Trans. TMS-AIME,* 1968, vol. 242, p. 814.
23. G. Kurdjumov and G. Sachs: *Z. Physik,* 1930, vol. 64, p. 325.
24. C. A. Dubé: Ph.D. Thesis, Carnegie Institute of Technology, 1948.
25. H. I. Aaronson: *Decomposition of Austenite by Diffusional Processes,* p. 387, Interscience Publishers, New York, 1962.
26. Ph. Maitrepierre: IRSID, France, unpublished research.
27. Ph. Maitrepierre, D. Thivellier, and R. Tricot: *Mém. Sci. Rev. Mét.,* 1973, vol. 70, p. 893.
28. S. Wakamatsu: *Tetsu to Hagané,* 1970, vol. 56, p. 136.
29. D. Henriet: IRSID, France, private communication.
30. C. C. McBride, J. W. Spretnak, and R. Speiser: *Trans. ASM,* 1954, vol. 46, p. 499.
31. M. E. Nicholson: *Trans. AIME,* 1954, vol. 200, p. 185.
32. P. E. Busby, M. E. Warga, and C. Wells: *Trans. AIME,* 1953, vol. 197, p. 1463.
33. G. M. Leak: *Metal Treat. and Drop Forging,* Jan. 1956, p. 21.
34. G. Henry, B. Thomas, and R. Tixier: Proc. of the 3rd International Con-

ference on the Strength of Metals and Alloys, Cambridge, England, August 1973, p. 568.
35. J. Davidson, P. Balladon, Y. Honnorat, and X. Wache: *Mém. Sci. Rev. Mét.*, 1973, vol. 70, p. 543.
36. S. R. Keown: *Scand. J. Metall.*, 1973, vol. 2, p. 59.
37. M. Ueno and T. Inoue: *Trans. I.S.I. Jap.*, 1973, vol. 13, p. 210.
38. D. Dulieu and J. J. Irani: *J. Iron Steel Inst.*, 1969, vol. 207, p. 308.
39. P. Coldren: Climax Molybdenum Company, Ann Arbor, Mich. Private communication.
40. M. Lucco-Borlera and G. Pradelli: *Metall. Ital.*, 1967, no. 11, p. 907.
41. M. Lucco-Borlera and G. Pradelli: *Metall. Ital.*, 1968, no. 2, p. 140.
42. G. R. Kegg and J. M. Silcock: *Scripta. Met.*, 1972, vol. 6, p. 1083.
43. P. H. Pumphrey and J. W. Edington: *Acta Met.*, 1974, vol. 22, p. 89.
44. K. N. Tu and D. Turnbull: *Acta Met.*, 1967, vol. 15, p. 1317.
45. H. I. Aaronson and H. B. Aaron: *Met. Trans.*, 1972, vol. 3, p. 2743.
46. R. C. Sharma and G. R. Purdy: *Met. Trans.*, 1973, vol. 4, p. 2303.
47. R. B. Nicholson: *Phase Transformations*, p. 269, American Society for Metals, Metals Park, Ohio, 1970.
48. R. A. Grange and H. R. Hribal: USS Technical Report 40.061-010 (1), June 1972.